

IV.C.3 Hydrogen Trapping through Designer Hydrogen Spillover Molecules with Reversible Temperature and Pressure-Induced Switching

Angela D. Lueking (Primary Contact), Jing Li, Cheng-Yu Wang, Yonggang Zhao, Haohan Wu, Qihan Gong

The Pennsylvania State University
120 Hosler Building
University Park, PA 16802
Phone: (814) 863-6256
Email: adl11@psu.edu

DOE Managers

Jesse Adams
Phone: (720) 356-1421
Email: Jesse.Adams@ee.doe.gov

Channing Ahn
Phone: (202) 586-9490
Email: Channing.Ahn@ee.doe.gov

Contract Number: DE-FG36-08GO18139

Subcontractor

Rutgers University, Piscataway, NJ

Project Start Date: January 1, 2009

Project End Date: June 30, 2014

Overall Objectives

- Synthesize designer microporous metal-organic frameworks (MMOFs) mixed with catalysts to enable H-spillover for H₂ storage at 300 K-400 K and moderate pressures
- Develop methods to reliably introduce catalyst into MMOFs
- Demonstrate spectroscopic evidence for hydrogen spillover

Fiscal Year (FY) 2014 Objectives

- Determine high-pressure stability of Cu₃(2,4,6-tris(3,5-dicarboxylphenylamino)-1,3,5-triazine)(H₂O)₃ (CuTDPAT)
- Finalize control tests and interpretation of spectroscopic data for identification of H binding sites to CuTDPAT populated via spillover
- Assess thermal stability of Pt-doped CuTDPAT in H₂
- Assess role of MMOF structural defects in propagating room temperature hydrogenation of CuTDPAT

- Reporting: Submit four research papers to peer-reviewed journals, finalize doctoral theses of two students, finish reporting requirements

Technical Barriers

This project addresses the following technical barriers from the Hydrogen Storage section of the Fuel Cell Technologies Office Multi-Year Research, Development and Demonstration Plan:

- (A) System Weight and Volume
- (D) Durability/Operability
- (E) Charging/Discharging rates
- (O) Lack of Understanding of Hydrogen Physisorption and Chemisorption
- (P) Reproducibility of Performance

Technical Targets

Technical targets for this project are listed in Table 1. The Go/No-Go milestones for this project are listed as follows.

1. Exceed 3.0 wt% reversible (<80°C, <30 minutes) hydrogen storage through the use of the “hydrogen spillover” mechanism, metal-organic framework (MOF) material, or a combination of the two as proposed at moderate temperatures and pressure (i.e. 300-400 K and 100 bar).
2. Demonstrate hydrogen spillover mechanism provides a means to increase ambient temperature hydrogen uptake of the MOF and/or carbon support by 50%.

FY 2014 Accomplishments

- Reproducibility: Demonstrated 2-7-fold increase in measurement sensitivity, i.e. within 0.05 wt% for a 100-mg sample. Published peer-reviewed paper [1] demonstrating improved adsorption methodology to minimize error due to experimental volume calibrations for low-density samples.
- Reproducibility: Demonstrated PB-doping technique maintains MMOF structure, surface area, and porosity. Retains structure at temperatures up to 20-25°C below the undoped MMOF material. (Published in peer-reviewed journal [2].)
- System Weight and Reproducibility: Demonstrated both MMOF structural defects and dissociation catalyst may increase room temperature H₂ adsorption (submitted to peer-reviewed journal).

TABLE 1. Progress towards Meeting Technical Targets for Hydrogen Storage

Characteristic	Units	2017 Target for Light-Duty Fuel Cell Vehicles	Status
Gravimetric Capacity	kg/kg	5.5 wt%	0.6-0.8 wt% (Uptake incomplete after 40-60 hours)
Durability/Operability Operating temperature	°C	-40/60	25°C tested
Charging/Discharging Rates System fill time	min	3.3	>80 Hours
Lack of Understanding of Physisorption versus Chemisorption	--	--	Chemisorption sites identified via spectroscopy, Reversible dehydrogenation between 25-125°C.
Reproducibility of Performance	--	--	Method to introduce catalytic sites into MMOFs developed; reproducible at low pressure. Thermal stability of MMOF retained after catalytic doping. MMOF studied is unstable at high-pressure (even prior to catalyst addition).

- Lack of Understanding of Physisorption vs. Chemisorption: Identified three chemisorption sites on CuTDPAT MMOF populated via high-pressure hydrogen spillover. Spectroscopic identification confirmed with theoretical calculations. (Submitted to peer-reviewed journal.)



INTRODUCTION

The term hydrogen spillover has been used to describe a synergistic effect between high-surface area adsorbents and associated catalysts. The associated catalyst dissociates molecular H₂ into atomic H species, which may then diffuse to and chemisorb to the support. This process occurs at moderate temperature (i.e. 300 K) and may lead to a much higher uptake than expected for the metal catalyst or high-surface area adsorbent alone under comparable conditions. Spillover materials using MMOFs have been reported to

have high uptake at ambient temperature: bridged ('br') PtAC/IRMOF8 (AC=activated carbon) achieved 4 wt% excess adsorption at 100 bar and 298 K [3]. (The structure of IRMOF8 is illustrated in Figure 1A.) Independent groups have demonstrated up to 4.2 wt% at 6.9 MPa after extended equilibration for brPtAC/IRMOF-8 [4]. Subsequent reports on spillover materials at room temperature have varied from less than physisorption to almost 9 wt%, demonstrating difficulties in reproducibility and invoking controversy. These uptakes approach DOE goals at ambient temperature; however, as the process is highly dependent upon synthesis, measurement, and catalytic particle size, [5,6] the process remains poorly understood. It is anticipated that optimization of the MMOF structure, surface chemistry, and porosity will further increase uptake via spillover. Meeting DOE hydrogen storage targets at moderate temperature will have significant engineering advantages for mobile applications, as temperature of operation has implications for system weight.

In prior years of this project, we have developed and tested some 20 new MMOF structures with incorporated

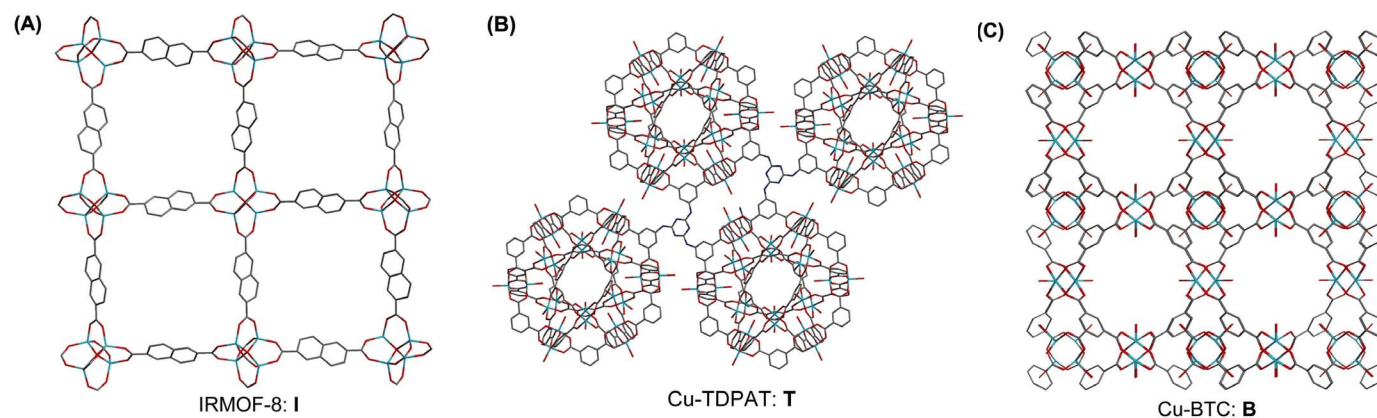


FIGURE 1. Diagram of IRMOF8 (I), CuTDPAT (T), and CuBTC (B), in which zinc (for I) and copper paddlewheel (for T and B) structure work as metal clusters, while the organic ligand (I: 2,6-naphthalenedicarboxylate, T: TDPAT, B: BTC) connects with metal cluster to form the long-range order MOF structure. TDPAT contains nitrogen in the center rings as well as three branches stretching from the center ring, similar to melamine. (Gray: C, Red: O, Cyan: Cu or Zn, Blue: N)

catalysts, determined MMOF stability after various catalytic doping techniques, worked to reproducibly optimize the uptake of carbon-based Pt/AC catalysts, developed techniques to verify spillover to specific surface sites on MMOFs with spectroscopy, conducted extensive reproducibility tests on standard samples including the effect of measurement, synthesis, and pretreatment conditions, and quantitatively validated our differential adsorption measurement. In FY 2013, CuTDPAT (Figure 1B) was selected for more extensive studies due to its structure, stability, and baseline H₂ uptake at 300 K (0.61 [excess] and 1.04 [total] wt%, at 298 K and 60 bar, measured by Rutgers University). CuTDPAT is the smallest member of (3,24)-connect nets of *rht* topology made of a three-armed hexacarboxylate ligand and 24 M₂(COO)₄ paddle-wheel based supramolecular building blocks. The CuTDPAT framework is highly porous and contains three different types of cages, cuboctahedron, truncated tetrahedron, and truncated octahedron. The pore volume, Brunauer-Emmett-Teller (BET) and Langmuir surface areas are estimated to be 0.93 cc/g, 1,938 and 2,608 m²/g, respectively, calculated from N₂ adsorption isotherms at 77 K. CuTDPAT is featured with a high density of both open metal sites (1.76/nm³) and Lewis basic sites (3.52/nm³), as well as high thermal and water stability.

APPROACH

The project relates to materials development and optimization of catalyst, surface chemistry, crystal and pore structure, and system parameters for the hydrogen spillover phenomenon. For surface chemistry, three different MMOFs were doped with catalyst to test hydrogen storage and the effect of functional groups, namely IRMOF8, CuTDPAT, and Cu₃(1,3,5-benzenetricarboxylate [BTC])₂(H₂O)₃ (CuBTC) (see Figure 1). Novel methods to incorporate a hydrogen dissociation catalyst into MMOFs were evaluated, by focusing on methods that lead to well dispersed catalytic entities without compromising the original pore structure and surface area of the MMOF. The current ‘pre-bridge’ (PB) technique is adapted from methods published previously [7,8] with adaptation to use an optimized hydrogenation catalyst and MMOFs with various structures and surface chemistry. Hydrogen uptake is quantified utilizing both gravimetric and differential volumetric adsorption methods (detailed elsewhere [1]); the former allows for precise catalyst activation whereas the latter allows for high-pressure measurements and is more accurate than conventional volumetric techniques. Complementary spectroscopic techniques are being used to identify the active sites that bind with spilled over hydrogen.

RESULTS

In FY 2013, we reported successful insertion of a Pt/AC catalyst was inserted into CuTDPAT via a solvothermal PB

doping technique [7,8], with almost complete retention of surface area and structure for four preparations. At 1 bar and 298 K, the hydrogen uptake of PB-CuTDPAT was enhanced 7.8-fold relative to the ‘as-received’ CuTDPAT (i.e. 4.9 cc/g versus 0.6 cc/g for CuTDPAT), and the increase was attributed to hydrogen spillover from the catalyst to the CuTDPAT substrate. Low-pressure 300 K isotherms were reversible and cyclable. Spectroscopic results confirmed hydrogenation of N groups on the TPAT ligand. At high-pressure (70 bar), the uptake of PB-CuTDPAT exceeded that of the undoped CuTDPAT precursor for five measurements, but the uptake was less than ~1 wt% (excess) after 40-60 hours (but still increasing), demonstrating slow kinetics would render this material unsuitable for meeting DOE targets (see Table 1). Subsequent testing demonstrated undoped CuTDPAT was unstable in high-pressure hydrogen, which may have contributed to the slow adsorption kinetics.

As PB-CuTDPAT did not meet targets, and ultimately undoped CuTDPAT was not stable in high-pressure H₂, the focus in FY 2014 has been on reproducibility and mechanistic studies to better understand the hydrogen spillover mechanism for potential application to other substrates. Specifically, our focus in FY 2014 has turned to (I) a more mechanistic understanding of the hydrogen spillover process (Technical Barrier O), and (II) determining how the PB doping technique alters the thermal stability and structural integrity of MMOFs (Technical Barrier P) so that the technique could possibly be applied to future material development. Topic I has included (A) extensive analysis of spectroscopic data and micrographs of three PB-MOF materials after hydrogenation, (B) control tests to ascertain the role of introduced defects on the 300 K enhancement, and (C) development/implementation of methodology to assess structural defects in Cu-type MOFs in order to quantify their effect on 300 K hydrogen uptake. Topic II has included: (D) thermal stability testing of IRMOF8 and CuTDPAT doped via the ‘pre-bridge’ doping methodology, and (E) additional characterization tests of PB-CuTDPAT, PB-IRMOF8, and PB-CuBTC to ascertain the effect of surface chemistry and structure on spillover. Each of these subtasks is summarized briefly in subsequent paragraphs.

(O) Lack of Understanding of Hydrogen Physisorption and Chemisorption

IA: Analysis of Spectroscopic Data for PB-MOFs.

In FY 2013, we reported X-ray photoelectron spectra (XPS) demonstrating reversible (at T <400 K) hydrogenation of the N surface sites in PB-CuTDPAT after H₂ exposure at 70 bar. This reversible N hydrogenation was not observed in undoped CuTDPAT after H₂ exposure at any temperature or pressure studied. With more extensive analysis, we were able to assign the XPS features specifically to (1) the sp² N aromatic heterocycles in the center ring, and (2) the secondary-amine type NH in the branches (as detailed in Ref. Wang 2014a).

The latter assignment led us to revisit density functional theory (DFT) model calculations suggesting hydrogenation at this site was endothermic for the TDPAT ligand, and we were able to resolve this apparent discrepancy by considering the potential role of defects and charged ligands in the CuTDPAT structure. This demonstrates experimental and theoretical studies must be done in concert, as ultimately, truncated or analog model structures may not represent real materials. Experimentally, additional evidence for hydrogen chemisorption within CuTDPAT was found at (3) the Cu-O-C bond that connects the TDPAT ligand to the Cu paddlewheel. (A fourth potential binding site was the carbon atoms present in the TDPAT ligand, but the characterization techniques were relatively insensitive to C-H modes.) Subsequent DFT calculations identified hydrogenated Cu paddlewheel structures that were consistent with the experimental results, and exothermic with respect to molecular H₂.

Overall, these spectroscopic techniques provided evidence for hydrogenation of the TDPAT ligand at 300 K without full dissociation of CuTDPAT to Cu metal and H₆TDPAT, and provided strong support for the hydrogen spillover mechanism, as comparable hydrogenation was not observed in the absence of the Pt catalyst. The ability to detect hydrogenation sites with ex situ characterization techniques confirmed hydrogen spillover is a hydrogenation process, consistent with our previous results for carbon-based materials, including reversible (at 300 K) hydrogenation identified with in situ spectroscopy [9], and detailed DFT calculations [9,10]. Interestingly, spectroscopic evidence of hydrogenation of the TDPAT ligand was observed only after higher pressure (70 bar) H₂ exposure, consistent with several previous experimental isotherms found in

the literature showing hydrogen spillover isotherms may not plateau at pressures up to 10 MPa. Combined with the partial degradation of CuTDPAT observed after high-pressure measurements, as well as the DFT calculations that demonstrate exothermic hydrogenation of N sites only for a charged ligand, the observed high-pressure hydrogenation may be associated with defect creation.

IB: Role of Defects to Enhance 300 K Hydrogen Chemisorption. To further explore the potential role of MOF structural defects in the enhanced hydrogen uptake of PB-CuTDPAT, AC-T was prepared as an analog to PB-CuTDPAT, but the Pt transition metal was excluded. In other words, the AC support was inserted into the CuTDPAT structure during synthesis, omitting the Pt nanoparticles on the Pt/AC catalyst that was inserted into PB-CuTDPAT. At 1 bar and 300 K, the hydrogen excess adsorption of AC-T exceeded that expected for physisorption to its components by a factor of 4, whereas the uptake of PB-CuTDPAT exceeded that expected for physisorption by a factor of 8 (Figure 2A). This strongly suggests defects play a role in enhancing the room temperature uptake, however, we cannot rule out the effect of Pt as the textural properties of AC-T were generally more favorable than PB-CuTDPAT for both physisorption (i.e. the BET surface area was higher) and hydrogenation of external crystallite edge sites (based on external surface area determinations, XPS, X-ray diffraction (XRD), and electron micrographs). As mentioned above, complementary DFT calculations demonstrate N hydrogenation of the NH amine sites on the H₆TDPAT is highly endothermic, whereas hydrogenation of a charged H₆TDPAT ligand is exothermic. Similarly, previous calculations demonstrated structural defects would propagate the hydrogen spillover

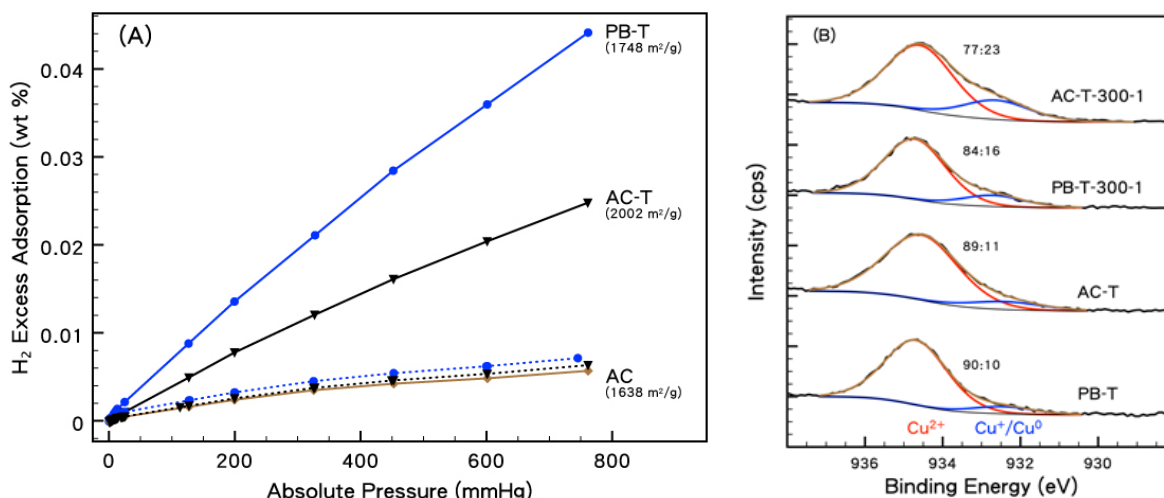


FIGURE 2. (A) Hydrogen 300 K 1 bar excess isotherms of Maxsorb AC, AC in Cu-TDPAT (T) via PB method (AC-T), and pre-bridged Cu-TDPAT with Pt/AC (PB-T), with expected uptake (dotted lines) based on weighted average versus experimental data (solid line). (B) The XPS spectra of Cu 2p 3/2 of AC-T and PB-TDPAT, before (bottom two) and after (top two) hydrogen exposure at 300 K and 1 bar, demonstrates reduction of Cu after mild H₂ exposure, which is more pronounced for AC-T.

mechanism via a hole-mediated effect [11]. Perhaps notably then, the Cu paddlewheel showed reduction after 300 K, 1 bar exposure, and the effect was more pronounced for AC-T than for PB-TDPAT (Figure 2B). The reduction of the Cu paddlewheel may be associated with partial charging of the ligand, resulting in more thermodynamically favorable hydrogenation of the ligand.

IC: Further Characterization of Defects. The potential increase in 300 K hydrogen adsorption by the introduction of defects and/or partial ligand charging of AC-T required further experimental validation. However, the readily available characterization methods (i.e. XPS, Fourier transform infrared [FTIR], XRD, and N_2 physisorption) were relatively insensitive probes of MMOF defects. Although Cu XPS demonstrated some reduction after H_2 exposure for AC-T (Figure 2B), and this has been associated with defects [12], this technique is not a well-established probe of defects in Cu-paddlewheel MOFs. Thus, we attempted to extend in situ FTIR probes of CO adsorption to CuBTC [12-14] to CuTDPAT, as both have the same Cu paddlewheel building unit. However, the CO signal in FTIR after CO adsorption/desorption to CuTDPAT at 150 K was notably different than adsorption to CuBTC controls that were conducted in parallel measurements. Whereas CO adsorption to CuBTC gave rise to perturbation of the CO spectra at $\sim 2,170$ and $\sim 2,120$ cm^{-1} (which are associated with adsorption at Cu^{2+} axial positions and defect sites, respectively [12-14]), both of these features were absent in CuTDPAT at all conditions studied. Additional control studies ruled out the effect of retention of the coordinated solvent, pretreatment conditions, sample preparation conditions, and thermal degradation. It seems that the lack of CO perturbation in CuTDPAT is associated with either the electron withdrawing nature of the TDPAT ligand (vs. the BTC ligand in CuBTC) or the equilibrium distance between CO and the Cu Paddlewheel site, which would be affected by differences in porosity of the two Cu-type MOFs. Thus, a more quantitative assessment of the role of introduced or induced defects on 300 K H_2 adsorption to CuTDPAT was not possible before project conclusion.

(P) Reproducibility of Performance

IID: Thermal Stability. As discussed above, CuTDPAT was degraded in high-pressure H_2 , even prior to introduction of a catalyst. Although PB-CuTDPAT was ultimately found not to be a good candidate to meet DOE targets, we were interested in whether the PB doping technique may be used for other MMOFs (or other porous coordination polymers), and the effect the doping would have on the thermal stability of the materials. We compared the thermogravimetric analysis profiles of PB-CuTDPAT and PB-IRMOF8 to their undoped counterparts, in both N_2 and H_2 , and found the PB doping technique had only a modest effect on the thermal stability of these two MMOFs. In brief, the onset of thermal degradation was reduced by 10-25 K, relative to the undoped

MMOF precursor. PB-IRMOF8 was stable up to 660 K in H_2 (vs. 680 K for IRMOF8) and weight loss was $<0.1\%/hr$ at 573 K in long time (i.e. 5 hr) experiments. PB-CuTDPAT was stable up to 540 K in H_2 (vs. 550 K for CuTDPAT) and weight loss was $<0.1\%/hr$ in the long term stability tests up to 473 K. However, despite apparent thermal stability at 473 K, PB-CuTDPAT exhibited a loss of BET surface area after heating to 473 K. Additional evidence for hydrogen chemisorption to PB-CuTDPAT was found in these tests, and likely contributed to the observed decrease in BET surface area.

III: Role of Other Parameters in Reproducibility of 300K H_2 Adsorption in Catalyzed MMOFs. At project onset, the primary goal of this project was to investigate the role of surface chemistry and porosity on enhancing hydrogen uptake in catalyzed MMOFs via hydrogen spillover. Due to reproducibility issues in the broader field, however, the project was restructured in Year 2 to focus more on reproducibility and validation of the spillover mechanism, with a focus on one particular MMOF (namely, CuTDPAT). As we return to the initial question at project conclusion, we find that surface chemistry and porosity play a secondary role to catalyst-MMOF connectivity. This is illustrated by the comparison of the low pressure 300 K isotherm of three MMOFs (IRMOF8, CuBTC, and CuTDPAT), all doped with Pt/AC via the PB doping technique. Although the surface chemistry and structure of these three MMOFs are very different (see Figure 1 A-C), these factors played very little role in dictating the hydrogen isotherms.

Specifically, the hydrogen isotherms at 300 K of the PB-MOF composites (solid lines, Figure 3A) are compared to the weighted average of their components (dotted lines, Figure 3A). The PB-CuTDPAT and PB-IRMOF8 samples show significant enhancement in hydrogen uptake relative to those of the weighted average of their components, whereas PB-CuBTC mirrors the uptake expected from the weighted average. In fact, the hydrogen uptake of PB-CuTDPAT at 1 bar exceeds (by $\sim 25\%$) that of Pt/AC, despite having a fraction ($\sim 1/20^{th}$) of the introduced catalyst. Furthermore, the slope of the H_2 isotherms for PB-CuTDPAT and PB-IRMOF8 are increased relative to the undoped precursors. These effects cannot be attributed to surface chemistry or porosity; rather, they correlate to observations of catalyst encapsulation via visual microscopy, increased mesoporosity (as determined from N_2 adsorption), and slightly expanded d-spacing in the XRD of PB-CuTDPAT and PB-IRMOF8. In contrast, the lack of enhancement seen for PB-CuBTC can be attributed to the fact that the Pt/AC catalyst was not effectively incorporated into the CuBTC matrix, judging from the optical microscopy, XRD, and decreased N_2 adsorption. We believe this is due to the smaller particle size of the methodology used to produce CuBTC. To better quantify this enhancement, we introduce a spillover efficiency parameter, η , defined as:

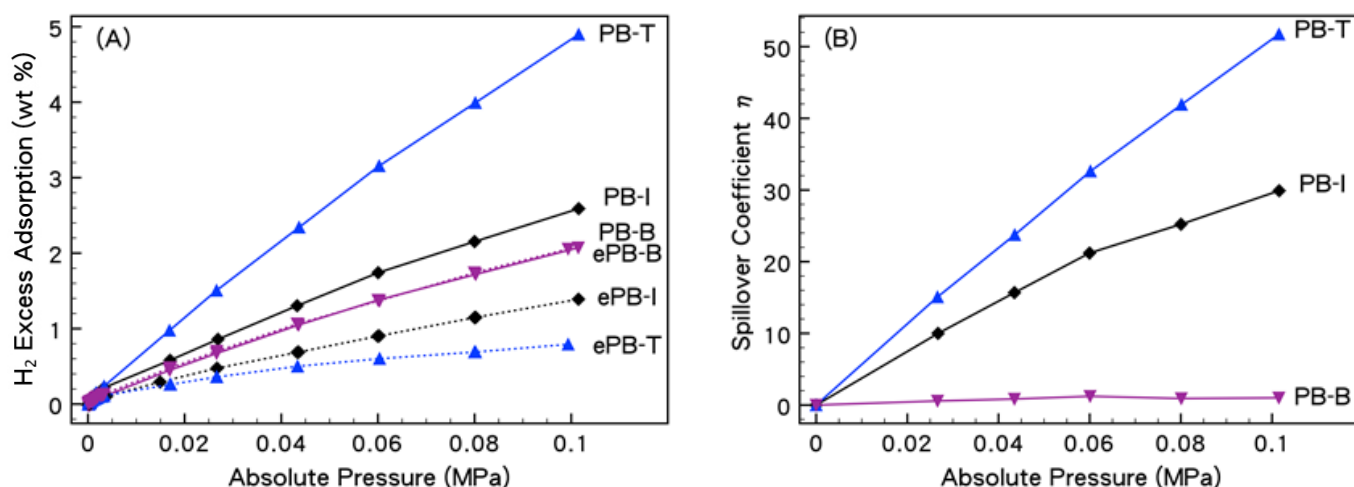


FIGURE 3. (A) Hydrogen 300 K 1 bar excess isotherms of expected (dotted line) PB-MOF samples vs. experimental data (solid line). The expected isotherms are shown based on the weighted average of each component in the composite. (B) Spillover efficiency η (see Eq 1) at 300 K of pre-bridged MOFs. Sample names have been abbreviated as PB-T, PB-I, and PB-B for PB-CuTDPAT, PB-IRMOF8, and PB-CuBTC, respectively.

$$\eta \equiv \frac{H}{M_S} = \frac{H}{M_T \cdot D} = \frac{\mu}{D} \quad \text{Equation 1}$$

Where H is the amount of hydrogen adsorbed above and beyond adsorption to the components measured independently, M_S is the active Pt surface metal determined from H₂ measurements of the corresponding Pt/AC, M_T is the total Pt metal content, and D is the dispersion of the metal (i.e. ratio of surface sites to total metal atoms). A spillover efficiency exceeding 1 would be an indication of hydrogen spillover, and use of the active metal sites in its calculation helps to account for differences between the activities of the Pt/AC catalysts used in the synthesis of the different materials. The data clearly shows PB-CuTDPAT has the highest spillover efficiency, whereas the spillover effect in PB-CuBTC is negligible. For PB-TDPAT and PB-IRMOF8, spillover efficiency increases with pressure, suggesting greater access of H to the MMOF at increased pressure. The increased spillover efficiency seen for PB-TDPAT and PB-IRMOF8 may be associated with porosity, as PB-TDPAT shows broad pore size distribution from 8-20 Å, and this has previously been associated with H₂ transport to the catalyst [15-18] with a particular emphasis on pores within a fractal network that are greater than 3.2 nm [19]. Large pores would facilitate gaseous H₂ diffusion to the catalyst and subsequent spillover; in contrast, gaseous H₂ diffusion to catalysts embedded in micropores would be slowed.

The high uptake of PB-TDPAT (relative to PB-IRMOF8) cannot be attributed to surface chemistry, as DFT predictions actually indicate the chemical functionalities of the H₆TDPAT ligand are unfavorable for hydrogen diffusion and hydrogenation [20]. The textural properties of CuTDPAT and IRMOF8 do not differ enough to warrant the differences seen

in the H₂ uptake, and the surface areas are similar (BET = 1,640 and 1,380 m²/g, respectively). Thus, it seems likely that the high uptake seen for PB-CuTDPAT is associated with the creation of defects, and complementary XPS results suggest this structure is particularly susceptible to defect formation. Furthermore, the uptake can be completely eliminated, as in the case of PB-CuBTC, by insufficient catalyst-MMOF contact, which has been emphasized previously.

CONCLUSIONS AND FUTURE DIRECTIONS

- A PB doping technique reproducibly incorporated catalytic entities into MMOFs, while retaining structure and textural properties of the MMOF. The thermal stability of the MMOF was within 10-25 K of the precursor (for IRMOF8 and CuTDPAT).
- The PB technique led to reproducible hydrogen uptake at low pressure for two MMOFs (IRMOF8, CuTDPAT). The high H₂ uptake of PB-CuTDPAT was attributed to both the creation of defects and the introduction of Pt catalyst. Porosity, surface area, and/or surface chemistry of the MMOF did not correlate to high hydrogen uptake. Enhancement due to hydrogen spillover was eliminated when there was insufficient contact between the inserted catalyst and the MMOF (for PB-CuBTC).
- At high pressure, the uptake of PB-CuTDPAT exceeded that of the CuTDPAT precursor in five cases, but was extremely slow (i.e. in excess of 20-40 hours). Further tests at high pressure for CuTDPAT were aborted due to inherent mechanical instability of CuTDPAT (even prior to catalytic doping) in H₂.
- Spectroscopic evidence for hydrogen spillover to PB-CuTDPAT showed hydrogenation of the TDPAT ligand

and the Cu-O-C site, verifying the hydrogen spillover mechanism, and further demonstrating hydrogen spillover occurs through the process of weak chemisorption.

The project concluded on June 30, 2014. Open issues remaining include:

- Introduced or inherent defects within MMOF play a pivotal role in 300 K hydrogen uptake, and may contribute to propagation of hydrogen introduced via a catalyst. We were not fully able to quantify defects within the project timeframe, due to unexpected results when a probe of defects was extended from CuBTC to CuTDPAT.
- More direct contact between the inserted catalyst and the substrate (which acts as a reservoir for hydrogen) would be needed to overcome the slow kinetics observed at high pressure. Yet, prior studies from our laboratory suggest many ‘traditional’ methods to catalytically dope MMOFs lead to structural degradation of the MMOF.
- Thus, it is difficult to see how reproducible hydrogen uptake via spillover will be achieved with MOFs doped with transition metals. Perhaps catalytic sites could be incorporated directly into the MMOF framework. Or, novel metal-carbon structures may be more appropriate. For reversible hydrogen uptake, a hydrogenation reaction with a small ΔG (Gibbs Free Energy) is required, but unique to hydrogen spillover, the activation energy for surface diffusion from each surface site must also be considered in material design. A theoretical study of ~20 model surfaces demonstrates the relationship between surface binding energy and the barrier for diffusion are not correlated [10], contrary to common “rules of thumb” in the literature. (However, these rules of thumb serve to provide initial estimates to correlate the two parameters.)
- It is not clear why the rates of hydrogen spillover were impeded at high pressure (for PB-CuTDPAT), but this was observed in previous reports in this field as well. Once again, the barrier for surface diffusion must be considered in the design of hydrogen spillover materials.

FY 2014 PUBLICATIONS/PRESENTATIONS

1. Wang, C.Y., Gray, J.L., Gong, Q., Zhao, Y., Li, J., Klontzas, E., Psfogiannakis, G., Froudakis, G., Lueking, A.D., “Hydrogen Storage with Spectroscopic Identification of Chemisorption Sites in Cu-TDPAT via Spillover from a Pt/Activated carbon catalyst”, *J. Phys. Chem. C.*, Submitted 2014.
2. Sircar, S., Pramanik, S., Li, J., Cole, M., Lueking, A.D., Corresponding States Interpretation of Adsorption in Gate-Opening Metal-Organic Framework Cu(dhbc)2(4,4i-bpy), *J. Phys. Chem. C.*, Submitted, 2014.
3. Sircar, S., Lueking, A.D., Adsorption Rates in Gate-Opening Metal Organic Frameworks: Development of a Combined Relaxation and Diffusion Model”, *Langmuir*, Submitted, 2014.

4. Wang, C.Y., Gong, Q., Zhao, Y., Li, J., Lueking, A.D., “Stability and Catalytic Activity of Metal-Organic Frameworks Prepared via Different Catalyst Doping Methods”, *J. Catal.*, 2014, In Press.

5. Sircar, S., Wang, C.Y., Lueking, A.D., “Design of High Pressure Differential Volumetric Adsorption Measurements with Increased Accuracy”, *Adsorption*, 19 (6), 1211-1234, 2013. DOI: 10.1007/s10450-013-9558-8.

REFERENCES

1. Sircar, S.; Wang, C.-Y.; and Lueking, A.D. *Adsorption*. **2013**, 1-24.
2. Wang, C.Y.; Gong, Q.; Zhao, Y.; Li, J.; and Lueking, A.D. *J. Catal.* **2014**.
3. Li, Y. and Yang, R.T. *J. Am. Chem. Soc.* **2006**, 128, 8136-8137.
4. Tsao, C.S.; Yu, M.S.; Wang, C.Y.; Liao, P.Y.; Chen, H.L.; Jeng, U.S.; Tzeng, Y.R.; Chung, T.Y.; and Wu, H.C. *J. Am. Chem. Soc.* **2009**, 131, 1404-1406.
5. Stadie, N.P.; Purewal, J.J.; Ahn, C.C.; and Fultz, B. *Langmuir*. **2010**, 26, 15481-15485.
6. Stuckert, N.R.; Wang, L.; and Yang, R.T. *Langmuir*. **2010**, 26, 11963-11971.
7. Yang, S.J.; Cho, J.H.; Nahm, K.S.; and Park, C.R. *Int. J. Hydrogen Energ.* **2010**, 35, 13062-13067.
8. Lee, S.Y. and Park, S.J. *Int. J. Hydrogen Energ.* **2011**, 36, 8381-8387.
9. Liu, X.M.; Tang, Y.; Xu, E.S.; Fitzgibbons, T.C.; Larsen, G.S.; Gutierrez, H.R.; Tseng, H.H.; Yu, M.S.; Tsao, C.S.; Badding, J.V.; Crespi, V.H.; and Lueking, A.D. *Nano Lett.* **2013**, 13, 137-41.
10. Lueking, A.D.; Psfogiannakis, G.; and Froudakis, G.E. *J. Phys. Chem. C.* **2013**, 117, 6312–6319.
11. Lee, K.; Kim, Y.H.; Sun, Y.Y.; West, D.; Zhao, Y.; Chen, Z.; and Zhang, S.B. *Physical Review Letters*. **2010**, 104, 236101.
12. St Petkov, P.; Vayssilov, G.N.; Liu, J.; Shekhah, O.; Wang, Y.; Wöll, C.; and Heine, T. *Chemphyschem*. **2012**, 13, 2025-2029.
13. Drenchev, N.; Ivanova, E.; Mihaylov, M.; and Hadjiivanov, K. *Phys. Chem. Chem. Phys.* **2010**, 12, 6423-7.
14. Szanyi, J.; Daturi, M.; Clet, G.; Baer, D.R.; and Peden, C.H. *Phys. Chem. Chem. Phys.* **2012**, 14, 4383-90.
15. Li, Y. and Yang, R.T. *J. Phys. Chem. C.* **2007**, 111, 11086-11094.
16. Conner, W.C. and Falconer, J.L. *Chem. Rev.* **1995**, 95, 759-788.
17. Boudart, M.; Aldag, A.W.; and Vannice, M.A. *J. Catal.* **1970**, 18, 46-51.
18. Chen, H.; Wang, L.; Yang, J.; and Yang, R.T. *J. Phys. Chem. C.* **2013**, 117, 7565-7576.
19. Tsao, C.S.; Yu, M.S.; Chung, T.Y.; Wu, H.C.; Wang, C.Y.; Chang, K.S.; and Chen, H.L. *J. Am. Chem. Soc.* **2007**, 129, 15997-16004.
20. Wang, C.Y.; Gray, J.L.; Gong, Q.; Zhao, Y.; Li, J.; Klontzas, E.; Psfogiannakis, G.; Froudakis, F.; and Lueking, A.D. *J. Phys. Chem. C.* **2014**.